"©2011 IEEE. Personal use of this material is permitted. However, permission to reprint/republish this material for advertising or promotional purposes or for creating new collective works for resale or redistribution to servers or lists, or to reuse any copyrighted component of this work in other works must be obtained from the IEEE."

Aggregate Interference and System Performance in Finite Area Cognitive Radio Networks

Luxmiram Vijayandran, Prathapasinghe Dharmawansa†, Torbjörn Ekman and Chinthananda Tellambura‡
Department of Electronics and Telecommunications, Norwegian University of Science and Technology,
†Department of Electronic and Computer Engineering, Hong Kong University of Science and Technology,
‡Department of Electrical Engineering, University of Alberta.

***Abstract*—Interference management is a major issue in underlay cognitive radio networks. In this paper, we focus on characterizing the statistics of the aggregate interference experienced by a primary user and evaluate its performance through important metrics such as outage probability, bit error rate and amount of fading. In previous works, the infinite interferers area assumption prevailed since it mainly simplifies the analysis. In contrast, we investigate the more realistic finite area, and further consider various practical spatial configurations. Two of the possible applications the proposed finite reconfigurable model can advocate are the IEEE 802.22 (WRAN) digital TV scenario and the aggregate interference considering different path loss exponents. We first derive the exact moment generating function (MGF) of the interference, then quantify the mean, the variance, and the skewness. Subsequently, the primary system performances are evaluated leading to novel expressions based on the interference MGF.**

I. Introduction

In the last decade, cognitive radio (CR) technology [1] has become a popular candidate to overcome the increasing scarcity of the radio spectrum, by allowing the so-called secondary users (SUs) to opportunistically sense and utilize the available spectrum. In order to foster the CR paradigms, many important issues still need to be solved in different research areas. In particular, this work focuses on the theoretical analysis of the aggregate interference experienced by the primary system in an underlay CR network. This type of analysis can provide useful bounds for the interference level, and shed some light on the interplay between the interference behavior and different physical parameters (e.g., propagation characteristics, users density, area and power).

The characterization of the interference in different network configurations is crucial for the design of efficient interference management techniques. Although a well researched topic, the CR development has brought it again into the focus of researchers. The aggregate interference in a Poisson field of interferers was first studied in [2]. The interference was shown to follow a stable distribution with infinite variance. That work has then been extended to handle more practical issues such as: various type of channel fading (e.g., [3]–[5]), probability distribution approximations (e.g., [6], [7]), cell-based primary configuration (e.g., [8]), interferers using power control (e.g., [7]), or sensing capabilities (e.g., [6], [9]). The outage probabilities of the interfered nodes for various channels have been investigated in e.g., [4], [5]. The general approach which has hitherto been used to characterize the interference is first to evaluate its characteristic function (CF) (see e.g., [9]), then to apply the Fourier inverse transform to compute the probability distribution function (PDF). However, in practice, the CF may only be expressed at best with an integral form or does not have a closed-form solution for the inverse Fourier transform. The alternative way in practice is to numerically evaluate them or use approximation methods.

The aforementioned works and references therein undeniably provide very important results. Yet, they generally lack some practical requirements: First, most of them provide cumbersome expressions to handle without providing much insights; Second, and most importantly, they generally assume an unbounded area for the interferers for mathematical tractability. Valid approximation in various cases, such infinite models have however some practical limits. One cannot, for example, analyze the effect of the interferers from a specific targeted area around the interfered user. Moreover, those models are based on a unique path loss exponent (PLE) for any of the infinitely many interferers.

The main contributions of this work can be summarized in threefold: (i) To analyze the more realistic finite interferers area. Moreover, the configurable spatial model we consider enjoys wide applicability; (ii) To quantify different interference statistics in terms of the fundamental physical parameters and provide useful insights; (iii) To evaluate valuable performance metrics of the primary user (PU), such as outage probability, bit error rate and amount of fading. To fulfill these objectives, this work is mainly based on the powerful MGF approach.

The remainder of this paper is organized as follows: The system model with various settings is described in Section II. Section III provides the MGF and different key statistics of the interference. In section IV different PU performance metrics are evaluated. Finally, Section V concludes the paper.

II. System Model

We consider a primary cellular network composed of a base station (BS) at the center of the cell and PU receivers located anywhere within the cell. The secondary network lays outside the primary cell. This system model is depicted in Fig.1. We assume that both PUs and SUs use a single antenna, and their communications undergo path loss and Rayleigh fading. For tractability, we omit the shadowing effect. We aim at characterizing the statistics of the aggregate interference from SUs at any given PU and subsequently evaluate its

978-1-4577-1348-4/11/$26.00 ©2011 IEEE

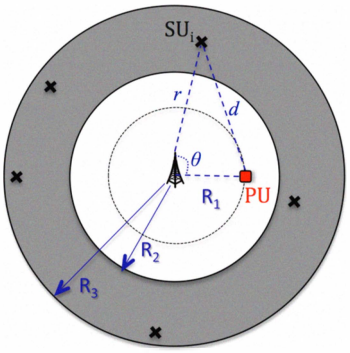

A	$R_1 \geq 0$	$R_2 \geq 0$	$R_3 \geq 0$
B	$R_1 = 0$	$R_2 \geq 0$	$R_3 \geq 0$
C	$R_1 = 0$	$R_2 = 0$	$R_3 \geq 0$
D	$R_1 = 0$	$R_2 = 0$	$R_3 \to \infty$

Fig. 1. System model and cases identification, defined by the three radii R_1, R_2 and R_3. The PU is symbolized by the square and the SUs by the crosses.

performances. Note that the PU being located anywhere in its cell, and not only at the center, the relative spatial distribution of the interferers around the PU is asymmetric (as in [8]), in contrast to the simple symmetric case as in most of the previous works e.g., [2], [3], [5]–[7], [9]

The system spatial parameters are defined by the three radii R_1, R_2 and R_3 such that $R_1 \leq R_2 \leq R_3$, where R_1 is the distance of the PU from its BS, and R_3 is the finite radius of the secondary network. R_2 can be simply defined as the primary cell radius (R_p), but can also account for an additional guard band around the primary cell [10] (i.e., $R_2 = R_p + \epsilon, \epsilon \geq 0$). Thus, PUs are within R_p, and SUs are beyond R_2.

One of the major applications of this model is the IEEE 802.22, digital TV (DTV) scenario [8], [11] i.e., the BS broadcasts the TV signal, the PUs are the TV receivers, and the CR network is the opportunistic system. Furthermore, in addition to characterize the interference from a specific region, the finite model allows to consider interference regions with different PLE (i.e., by successively varying the 3 radii configuration and computing the interference in each area with different PLE, and finally summing up). The two-ray model [12] is a simple example. Clearly, this more general finite spatial model is easily reconfigurable to obtain a spectrum of different network structures, thus enjoying wide applicability.

In practical scenarios, only statistical knowledge of the interferers location is available. Thus, following [2], we may as well treat them as completely random according to a homogeneous Poisson point process (PPP) in the two dimensional plan. The probability of N SUs being inside a region depends only on the total area and follows a Poisson distribution with mean $\lambda\pi R_{32}$, where $R_{32} = (R_3^2 - R_2^2)$ and λ characterizes the SUs density per unit area. This elegant theory provides a tractable and practical model and has prevailed in many works e.g., [2], [3], [5]–[7], [9].

We assume that each SU has the same transmit power P_{SU}, decays according to the PL law, and undergoes independent identically distributed (i.i.d.) Rayleigh fading. Thus, the aggregate interference I at the PU can be defined as

$$I = \sum_{i=1}^{N} I_i = \sum_{i=1}^{N} P_{SU} d_i^{-\alpha} \left| h_{SU_i} \right|^2 \quad (1)$$

where I_i is the ith SU interference, d_i is the distance between the PU and the ith SU, α is the PLE, and $|h_{SU_i}|^2$ is the exponentially distributed power envelope with unit mean. We assume that $|h_{SU_i}|^2$ is independent of d_i.

In most practical cases, the PLE generally varies between 1.6 (e.g., hallways inside buidings) and 6 (e.g., dense urban environments) [12]. However, in this paper we restrict our analysis to the two most representative cases in literature with 2 (i.e., free space) and 4. Furthermore, we consider four different practical configurations in terms of the radii R_1, R_2 and R_3 as summarized in the table in Fig.1. Clearly, Case A is the most general setting which incorporates the three other cases: B, C and D. Notable configuration is Case D for $\alpha = 4$ which has been analyzed in e.g., [2], [3], [5], [9]. It is important to note that Case D is only applicable for $\alpha > 2$, since the interference tends to infinity for $\alpha \leq 2$ as $R_3 \to \infty$ [2].

III. Statistics of the Interference

In this section, we first derive the exact closed-form expressions for the MGF of the aggregate interference. Subsequently, they will be employed to evaluate different statistics of I.

A. Moment Generating Function of I

By definition, the MGF of the aggregate interference I in (1), for a specific PLE α, is [13] $\mathcal{M}_I^{(\alpha)}(s) = \mathbb{E}_I \{\exp(-sI)\}$. Since the number of SUs N is a poisson distributed random variable, $\mathcal{M}_I^{\alpha}(s)$ can be written as [2]

$$\mathcal{M}_I^{(\alpha)}(s) = \sum_{N=0}^{\infty} \mathbb{E}_I \{\exp(-sI)|N\} \frac{\exp(-\lambda\pi R_{32})(\lambda\pi R_{32})^N}{N!}. \quad (2)$$

The random variables I_i, $i = 1...N$, being i.i.d., we get $\mathbb{E}_I \{\exp(-sI)|N\} = \mathbb{E}_{I_i} \{\exp(-sI_i)\}^N = \left(M_i^{(\alpha)}(s)\right)^N$, where $M_i^{(\alpha)}(s) = \mathbb{E}_{I_i} \{\exp(-sI_i)\}$ is the individual interference MGF from any ith SU. Thus, (2) can be written as

$$\mathcal{M}_I^{(\alpha)}(s) = \exp\left(\lambda\pi R_{32}\left(M_i^{(\alpha)}(s) - 1\right)\right). \quad (3)$$

Since $M_i^{(\alpha)}$, the MGF of the ith interferer, is independent of i, in what follows, without loss of generality, we omit the index i. In our model, the randomness of each individual interference stems from two factors, the random distance (i.e., d), and the fading power envelope (i.e., $|h_{SU}|^2$). In the sequel, it is mathematically more convenient to use the polar coordinates (r, θ) instead of d, as defined in Fig.1. Thus, we employ henceforth the geometric relation $d(r,\theta) = \sqrt{r^2 + R_1^2 - 2rR_1\cos\theta}$. The individual interference MGF can be written as

$$M^{(\alpha)}(s) = \mathbb{E}_{r,\theta}\left\{\int_0^{\infty} \exp\left(-sP_{SU}d^{-\alpha}(r,\theta)x\right) f_{|h_{SU}|^2}(x)dx\right\} \quad (4)$$

where the PDF of the exponential distribution is defined as $f_{|h_{SU}|^2}(x) = \exp(-x)$. The inner integral in (4) can be represented using the MGF of an exponential distribution such that we obtain

$$M^{(\alpha)}(s) = \mathbb{E}_{r,\theta}\left\{\frac{1}{1+sP_{SU}d^{-\alpha}(r,\theta)}\right\}. \quad (5)$$

Note that the convergence of the inner integral in (4) is satisfied if $sP_{SU} > -d^{\alpha}(r,\theta)$. Thus, we may as well assume in the sequel that $s > 0$, since it always satisfies the inequality. Next, we need to carefully define the spatial distribution of the interferers in (5) in terms of r and θ. Since SUs are uniformly distributed in the circular area, the PDF of r is given by the ratio perimeter over area as [2] $f_R(r) = 2r/R_{32}$ for $r \in [R_2, R_3]$, and the angular distribution is uniformly distributed over $[0, 2\pi)$ i.e., $f_\theta(\theta) = 1/2\pi$. Using the PDF of r and θ, (5) can be written as

$$M^{(\alpha)}(s) = \frac{1}{\pi R_{32}}\int_{R_2}^{R_3}\int_{0}^{2\pi}\frac{r}{1+sP_{SU}\left(r^2+R_1^2-2rR_1\cos\theta\right)^{-\alpha/2}}d\theta dr. \quad (6)$$

This double integral in (6) seems intractable for an arbitrary value of α. However, it can be solved for the representative cases, $\alpha = 2$ and $\alpha = 4$, which we present through the following two propositions. Due to space constraints, we only sketch the key steps for the proof of Proposition 1, and the proof of Proposition 2 is omitted.

Proposition 1: The MGF of the aggregate interference at the PU, for $\alpha = 2$, is given by

$$\mathcal{M}_I^{(2)}(s) = \exp\left(-sP_{SU}\lambda\pi\ln\left|\Psi^{(2)}(s)\right|\right) \quad (7)$$

where

$$\Psi^{(2)}(s) = \begin{cases} \frac{\sqrt{4sP_{SU}R_1^2+(R_3^2-R_1^2+sP_{SU})^2}+(R_3^2-R_1^2+sP_{SU})}{\sqrt{4sP_{SU}R_1^2+(R_2^2-R_1^2+sP_{SU})^2}+(R_2^2-R_1^2+sP_{SU})} & \text{Case A} \\ \frac{R_3^2+sP_{SU}}{R_2^2+sP_{SU}} & \text{Case B} \\ \frac{R_3^2+sP_{SU}}{sP_{SU}} & \text{Case C.} \end{cases}$$

Proof: Using the transformation $v = \tan(\theta/2)$ and [14, eq. 2.172.c] in (6), we obtain the MGF for $\alpha = 2$ as

$$M^{(2)}(s) = 1 - \frac{2sP_{SU}}{R_{32}}\int_{R_2}^{R_3}\frac{r}{\sqrt{\left(r^2+\left(sP_{SU}-R_1^2\right)\right)^2+4sP_{SU}R_1^2}}dr. \quad (8)$$

Using two transformations, $v = r^2$ and ϕ such that $v + \xi = \tau\tan\phi$, (8) can be written as

$$\begin{aligned} M^{(2)}(s) &= 1 - \frac{sP_{SU}}{R_{32}}\int_{\arctan\left((R_2^2+\xi)/\tau\right)}^{\arctan\left((R_3^2+\xi)/\tau\right)}\sec\phi d\phi \\ &= 1 - \frac{sP_{SU}}{R_{32}}\ln\left|\frac{\sqrt{\tau^2+\left(R_3^2+\xi\right)^2}+\left(R_3^2+\xi\right)}{\sqrt{\tau^2+\left(R_2^2+\xi\right)^2}+\left(R_3^2+\xi\right)}\right| \end{aligned} \quad (9)$$

where $\xi = sP_{SU} - R_1^2$ and $\tau = \sqrt{4sP_{SU}R_1^2}$. Finally, substituting (9) into (3) yields the MGF in (7) Case A. Corresponding MGFs for Case B and C are obtained substituting R_1 and R_2 by the proper values. ■

Proposition 2: The MGF of the aggregate interference at the PU, for $\alpha = 4$, is given by

$$\mathcal{M}_I^{(4)}(s) = \exp\left(-\sqrt{sP_{SU}}\lambda\pi\Psi^{(4)}(s)\right) \quad (10)$$

where

$$\Psi^{(4)}(s) = \begin{cases} \arctan\left(\frac{R_3^2}{\sqrt{sP_{SU}}}\right) - \arctan\left(\frac{R_2^2}{\sqrt{sP_{SU}}}\right) & \text{Case B} \\ \arctan\left(\frac{R_3^2}{\sqrt{sP_{SU}}}\right) & \text{Case C} \\ \pi/2 & \text{Case D.} \end{cases}$$

Note that a closed-form expression for the general Case A for $\alpha = 4$ seems mathematically intractable. The result for $\alpha = 4$ Case D, which was already obtained in [3, eq.7] using the CF approach, boils down to the simplest expression. One of the salient highlights of our contributions are the novel MGF expressions for the remaining cases. Quick calculations reveal that as $s \to \infty$ the MGFs in (7) and (10), for any cases except Case D, lead to a non-zero finite value. Interestingly, there is a non-zero probability of having zero interference, a behavior inherently hidden by the infinite area assumed in previous works. Due to space constraints, further mathematical investigations will be presented in the extended journal version.

B. Cumulants of I

By invoking the central limit theorem (CLT), one may tempt to approximate the PDF of I with a Gaussian PDF. However simulations have shown (e.g., [5], [6]) that the PDF is positively skewed and thus deviates from normality. This stems from the fact that interferers very close to the receiver terminal contribute a disproportionately large amount of interference, thus limiting the CLT validity. Therefore, the key parameters to characterize I are: the mean, the variance and the skewness [6]. We now evaluate those statistics using the cumulants of I. By definition, the nth cumulant of I is [13]

$$\kappa_n^{(\alpha)} = (-1)^n\frac{d^n}{ds^n}\ln\mathcal{M}_I^{(\alpha)}(s)\Big|_{s=0}. \quad (11)$$

The first orders cumulants have straightforward relations with the mean, $\mu_I^{(\alpha)} = \kappa_1^{(\alpha)}$, the variance, $\sigma_I^{(\alpha)2} = \kappa_2^{(\alpha)}$, and the skewness denoted by $\delta_I^{(\alpha)}$, such that $\delta_I^{(\alpha)} = E_I\left\{\exp\left((I-\mu_I)/\sigma_I\right)^3\right\} = (\kappa_3^{(\alpha)}/\kappa_2^{(\alpha)3/2})$. Substituting (7) or (10) in (11), the 1^{st}, 2^{nd} and 3^{rd} cumulants are computed following extensive algebraic manipulations with successive application of the L'Hôpital rule. For $\alpha = 2$, Case A and Case B are given as follows:

$$\kappa_1^{(2)} = \begin{cases} \lambda\pi P_{SU}\ln\left(\frac{R_3^2-R_1^2}{R_2^2-R_1^2}\right) & \text{Case A} \\ \lambda\pi P_{SU}\ln\left(\frac{R_3^2}{R_2^2}\right) & \text{Case B,} \end{cases}$$

$$\kappa_2^{(2)} = \begin{cases} \frac{2\lambda\pi P_{SU}^2\left\{R_3^4R_2^2-R_2^4R_3^2+R_1^4R_2^2-R_1^4R_3^2\right\}}{\left(R_2^2-R_1^2\right)^2\left(R_3^2-R_1^2\right)^2} & \text{Case A} \\ 2\lambda\pi P_{SU}^2\left(\frac{1}{R_2^2}-\frac{1}{R_3^2}\right) & \text{Case B,} \end{cases}$$

$$\kappa_3^{(2)} = \begin{cases} \frac{3\lambda\pi P_{SU}^3 g(R_1,R_2,R_3)}{\left(R_2^2-R_1^2\right)^4\left(R_3^2-R_1^2\right)^4} & \text{Case A} \\ \frac{3\lambda\pi P_{SU}^3\left(R_3^4-R_2^4\right)}{R_2^4R_3^4} & \text{Case B} \end{cases}$$

$$g(R_1,R_2,R_3)=2R_2^2R_1^2\left(R_3^2-R_1^2\right)^4-2R_3^2R_1^2\left(R_2^2-R_1^2\right)^4+2R_2^2R_3^2\left(R_2^2-R_1^2\right)^2\left(R_3^2-R_1^2\right)^2-2R_3^4\left(R_2^2-R_1^2\right)^4+R_2^4R_3^4\left(R_3^2-R_2^2\right)^2-2R_1^4R_2^2R_3^2\left(R_3^2-R_2^2\right)^2+R_1^8\left(R_3^2-R_2^2\right)^2.$$

Similarly, for $\alpha=4$, Case B is given as follows:

$$\kappa_1^{(4,B)}=\lambda\pi P_{SU}\left(\frac{1}{R_2^2}-\frac{1}{R_3^2}\right),$$
$$\kappa_2^{(4,B)}=\frac{2}{3}\lambda\pi P_{SU}^2\left(\frac{1}{R_2^6}-\frac{1}{R_3^6}\right),$$
$$\kappa_3^{(4,B)}=\frac{6}{5}\lambda\pi P_{SU}^3\left(\frac{1}{R_2^{10}}-\frac{1}{R_3^{10}}\right).$$

Those expressions can provide direct insights on the interplay between the interference and the different physical parameters. After careful inspection, several behaviors can be pointed out. It is easy to remark that Case C and D cannot be evaluated as the mean and the variance tend to infinity. This stems from the fact that when $R_2=R_1$, no protective region exists around the PU. Thus, there is a probability that a SU is exactly at the same position as the PU. In that situation the path loss model defined in (1) has a singularity and is generally not valid for $d<1$, as the wireless channel can not amplify the transmitted signal. Interestingly, the mean for $\alpha=2$ does not vary if we scale all the network spatial parameters by the same proportion. However, the variance changes. In contrast, for $\alpha=4$, both change. It is easy to see from $\kappa_1^{(2)}$ that if R_2 and R_3 are fixed and R_1 (i.e., PU) varies from the center of the cell to the edge, the mean increases much faster than with a linear trend. Thus, one can expect the performance of the primary cellular network, in average, to be much better than at the cell edge. It is also easy to note from $\kappa_1^{(2)}$ and $\kappa_1^{(4)}$ that for $\alpha=4$ one can set $R_3=\infty$, in contrast to $\alpha=2$ as the interference mean goes to infinity. This was already mentioned in [2], but without any quantification. In [6], general semi-analytical expressions for different type of channels are provided to compute the nth cumulant for Case D with $R_2=1$, $\forall\alpha>2$. Although useful, those integral expressions do not provide much insights and are not valid for Case A and B.

Figs. 2(a) and 2(b) compare the mean, the variance and the skewness between the analytical results and corresponding Monte-Carlo simulations averaged over 10^4 random simulations. The results are given for $\alpha=2$ and $\alpha=4$ with Case A and Case B, respectively. The curves between the simulations and the analytical expressions clearly match.

IV. PU System Performances

In this section we investigate the performance of the primary system through different metrics. We provide a closed-form expression for the outage probability. The bit error rate and amount of fading are given with single integral expressions.

A. Outage Probability (P_{out})

The outage probability is an important measure in determining the quality of service. By definition, $P_{\text{out}}(\gamma_{th})=\Pr(\gamma\leq\gamma_{th})$, where γ is the received signal-to-interference-noise-ratio (SINR), and γ_{th} is a predefined threshold. The average received power at the PU is defined as $P_{PU}=P_{PU}^{TX}R_1^{-\alpha}$, where P_{PU}^{TX} is the transmit power at the BS. Thus, PU's SINR, γ_{PU}, can be defined as

$$\gamma_{PU}=\frac{P_{PU}\left|h_{PU}\right|^2}{I+N_0} \tag{12}$$

where I is the aggregate interference due to SUs as defined in (1), N_0 is the noise variance and $\left|h_{PU}\right|^2$ is the exponential distributed power envelope with unit mean. In the sequel, without loss of generality, we assume a unit noise variance. Furthermore, we assume that $\left|h_{PU}\right|^2$ and I are independent. Based on (12), $P_{\text{out}}^{(\alpha)}(\gamma_{th})$ can be written as

$$P_{\text{out}}^{(\alpha)}(\gamma_{th})=\mathbb{E}_I\left\{F_{|h_{PU}|^2}\left(\frac{\gamma_{th}(I+1)}{P_{PU}}\right)\right\} \tag{13}$$

where the CDF of $\left|h_{PU}\right|^2$ is $F_{|h_{PU}|^2}(x)=1-\exp(-x)$. Finally, (13) can be written as

$$P_{\text{out}}^{(\alpha)}(\gamma_{th})=1-\exp\left(-\frac{\gamma_{th}}{P_{PU}}\right)\mathcal{M}_I^{(\alpha)}\left(\frac{\gamma_{th}}{P_{PU}}\right). \tag{14}$$

In (14), it is interesting to note that the PU's outage probability has a simple relation to the aggregate interference MGF.

Fig.2(c) illustrates the validity of (14). One can notice that for $\alpha=4$ and $R_2=500$m, the outage performance curves are very similar for R_3 equal to 1km and 2km. This stems from the fact that for hight PLE the interference behavior converges quickly in terms of radius. Thus, this can validate the theoretical infinite area assumption. However, this assumption becomes less valid for low PLE as shown by the performances of $\alpha=2$. One can observe that a larger distance of R_3 (i.e., $R_3>2$km) is required for the performance to converge compared to $\alpha=4$.

B. Bit Error Rate (BER)

Here, we investigate the important bit error rate metric. In particular, we focus on the coherent BPSK modulation for which the BER is defined as $P_b=\mathbb{E}_{\gamma_{PU}}\left\{Q\left(\sqrt{2\gamma_{PU}}\right)\right\}$. Instead of the classical Q-function expression, here it is convenient to use the alternate representation due to Craig i.e., $Q(x)=\frac{1}{\pi}\int_0^{\pi/2}\exp\left(-x^2/(2\sin^2\beta)\right)d\beta, x\geq 0$. Thus, P_b can be written as

$$P_b^{(\alpha)}=\frac{1}{2}\left(1-\sqrt{P_{PU}}\mathbb{E}_I\left\{\frac{1}{\sqrt{I+1+P_{PU}}}\right\}\right). \tag{15}$$

The next challenge is to evaluate the expected value in (15). To this end, we use the following relation

$$\frac{\Gamma(p)}{x^p}=\int_0^\infty v^{p-1}\exp\{-xv\}\,dv,\quad p>0,x>0 \tag{16}$$

where $\Gamma(p)$ is the gamma function. Finally, using (16) in (15) with $p=1/2$ (i.e., $1/\sqrt{x}=1/\sqrt{\pi}\int_0^\infty v^{-1/2}\exp\{-xv\}\,dv$), the BER for coherent BPSK can be written as

$$P_b^{(\alpha)}=\frac{1}{2}-\frac{\sqrt{P_{PU}}}{2\sqrt{\pi}}\int_0^\infty v^{-1/2}\exp\{-(1+P_{PU})v\}\mathcal{M}_I^{(\alpha)}(v)dv. \tag{17}$$

Fig.2(d) illustrates the validity of (17).

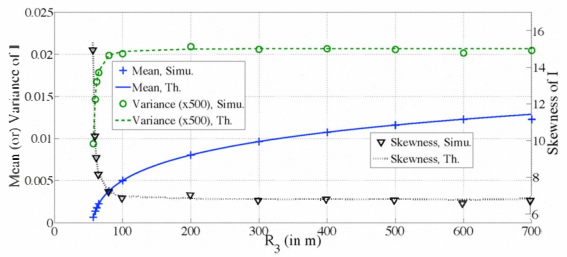

(a) Statistics of I: $\alpha = 2$; $R_1 = 50$m, $R_2 = 55$m and $P_{SU} = 30$dBm.

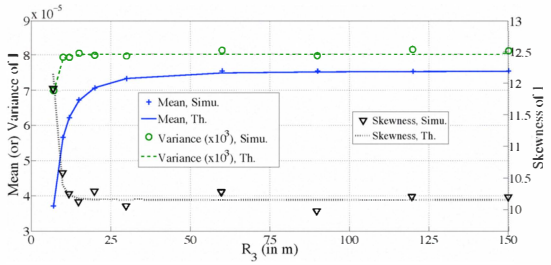

(b) Statistics of I: $\alpha = 4$; $R_1 = 0$m, $R_2 = 5$m and $P_{SU} = 30$dBm.

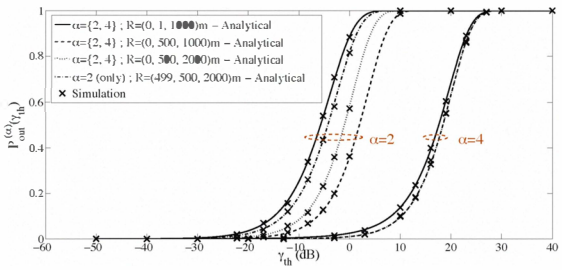

(c) Outage probability; $P_{SU} = 80$dBm

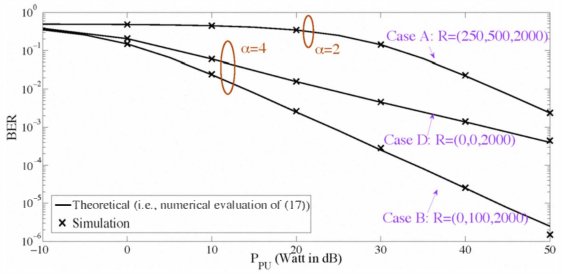

(d) BER for coherent BPSK; $P_{SU} = 90$dBm

Fig. 2. Illustration of the Monte-Carlo and analytical expressions correct match ($\lambda = 10^{-4}$).

C. Amount of Fading (AoF)

The AoF at the PU is an important performance measure which quantifies the severity of the fading channel. By definition, it is expressed as AoF $= \left(m_2 - m_1^2\right)/m_1^2$, where m_1 and m_2 are the first and second moments respectively. The 1^{st} moment can be written as

$$m_1^{(\alpha)} = \mathbb{E}_{\gamma_{PU}}\left\{\gamma_{PU}\right\} = P_{PU}\mathbb{E}_{|h_{PU}|^2}\left\{|h_{PU}|^2\right\}\mathbb{E}_I\left\{\frac{1}{I+1}\right\}. \quad (18)$$

Using (16) with $p = 1$, (18) yields $m_1^{(\alpha)} = P_{PU}\int_0^\infty \exp(-v)\mathcal{M}_I^{(\alpha)}(v)dv$. Similarly, m_2 can be written as $m_2^{(\alpha)} = \mathbb{E}_{\gamma_{PU}}\left\{\gamma_{PU}^2\right\} = 2P_{PU}^2\int_0^\infty v\exp(-v)\mathcal{M}_I^{(\alpha)}(v)dv$. We omit the figure illustration due to space constraint.

V. Summary and Conclusive Remarks

This paper has investigated the performance of a PU experiencing interference from a CR system. The system model we considered, with three configurable and finite radii, enjoys a wide practical applicability. By employing the powerful MGF tool, we have quantified different statistics of the aggregate interference and evaluated different performance metrics of the PU such as outage probability, bit error rate and amount of fading. Clearly, the theoretical infinite assumption may give reasonable approximations. However, this initial work reveals some interesting insights into the interference management. For instance, the mean for $\alpha = 2$ does not vary when scaling the whole network by the same proportion, and the probability of having zero interference is non-zero in finite PPP, a behavior inherently hidden by the infinite area assumption.

Acknowledgment

This work is performed in the SENDORA project, supported by EU under FP7.

References

[1] J. Mitola, "An Integrated Agent Architecture for Software Defined Radio," Ph.D. dissertation, Royal Institute Technology (KTH), Stockholm, Sweden, 2000.

[2] E. S. Sousa and J. A. Silvester, "Optimum transmission ranges in a direct-sequence spread-spectrum multihop packet radio network," *IEEE J. Sel. Areas Commun.*, vol. 8, no. 5, pp. 762–771, June 1990.

[3] M. Souryal, B. Vojcic, and R. Pickholtz, "Ad-hoc, multihop CDMA networks with route diversity in a Rayleigh fading channel," in *Proc. IEEE MILCOM*, Washington DC, Oct. 2001, pp. 1003–1007.

[4] X. Hong, C.-X. Wang, and J. Thompson, "Interference modeling of cognitive radio networks," in *Proc. IEEE VTC*, Singapore, May 2008, pp. 1851–1855.

[5] R. Dahama, K. W. Sowerby, and G. B. Rowe, "Outage probability estimation for licensed systems in the presence of cognitive radio interference," in *Proc. IEEE VTC*, Barcelona, Spain, Apr. 2009, pp. 1–5.

[6] A. Ghasemi and E. S. Sousa, "Interference aggregation in spectrum-sensing cognitive wireless networks," *IEEE J. Sel. Topics in Signal Process.*, vol. 2, no. 1, pp. 41–56, Feb. 2008.

[7] S. Singh, N. B. Mehta, A. F. Molisch, and A. Mukhopadhyay, "Moment-matched lognormal modeling of uplink interference with power control and cell selection," *IEEE Trans. Wireless Commun.*, vol. 9, no. 3, pp. 932–398, Mar. 2010.

[8] M. Vu and V. Tarokh, "On the primary exclusive region of cognitive networks," *IEEE Trans. Wireless Commun.*, vol. 8, no. 7, pp. 3380–3385, Jul. 2009.

[9] M. Z. Win, P. C. Pinto, and L. A. Shepp, "A mathematical theory of network interference and its applications," *Proc. IEEE*, vol. 97, no. 2, pp. 1–26, Feb. 2009.

[10] A. Hasan and J. G. Andrews, "The guard zone in wireless ad hoc networks," *IEEE Trans. Commun.*, vol. 6, no. 3, pp. 897 – 906, Mar. 2007.

[11] C. Cordeiro, K. Challapali, D. Birru, and S. Shankar, "IEEE 802.22: An introduction to the first wireless standard based on cognitive radios," *Journal of Communications*, vol. 1, no. 1, pp. 38–47, Apr. 2006.

[12] J. D. Parsons, *The Mobile Radio Propagation Channel, 2nd ed.* New York: Wiley, 2000.

[13] A. Papoulis and S. U. Pillai, *Probability, Random Variables, and Stochastic Processes, 4th ed.* New York: McGraw Hill, 2002.

[14] I. S. Gradshteyn and I. M. Ryzhik, *Tables of Integrals, Series and Products.* Academic Press, 1980.